

Neural Influence Estimator: Towards Real-time Solutions to Influence Blocking Maximization

Wenjie Chen, Shengcai Liu, *Member, IEEE*, Yew-Soon Ong, *Fellow, IEEE*, Ke Tang, *Fellow, IEEE*

Abstract—Real-time solutions to the influence blocking maximization (IBM) problems are crucial for promptly containing the spread of misinformation. However, achieving this goal is non-trivial, mainly because assessing the blocked influence of an IBM problem solution typically requires plenty of expensive Monte Carlo simulations (MCSs). Although several approaches have been proposed to enhance efficiency, they still fail to achieve real-time solutions to IBM problems of practical scales. This work presents a novel approach that enables solving IBM problems with hundreds of thousands of nodes and edges in seconds. The key idea is to construct a fast-to-evaluate surrogate model, called neural influence estimator (NIE), as a substitute for the time-intensive MCSs. To this end, a learning problem is formulated to build the NIE that takes the false-and-true information instance as input, extracts features describing the topology and inter-relationship between two seed sets, and predicts the blocked influence. A well-trained NIE can generalize across different IBM problems defined on a social network, and can be readily combined with existing IBM optimization algorithms such as the greedy algorithm. The experiments on 25 IBM problems with up to millions of edges show that the NIE-based optimization method can be up to four orders of magnitude faster than MCSs-based optimization method to achieve the same solution quality. Moreover, given a real-time constraint of one minute, the NIE-based method can solve IBM problems with up to hundreds of thousands of nodes, which is at least one order of magnitude larger than what can be solved by existing methods.

Index Terms—Influence blocking maximization, Monte Carlo simulation, surrogate model, neural network

I. INTRODUCTION

ONLINE social networks have become vital communication platforms for users; however, they have also emerged as breeding grounds for the spread of rumors and hate speech. According to the World Economic Forum, misinformation on social media has been recognized as one of the global risks in 2023 [1]. One commonly employed approach to mitigating the impact of misinformation is to distribute correct information to raise users' awareness and thus limit the spread of misinformation. This approach is commonly known as influence blocking maximization (IBM) in the social network community [2].

Wenjie Chen is with the School of Information Management, Central China Normal University, Wuhan 430079, P. R. China.

Shengcai Liu is with the Centre for Frontier AI Research (CFAR), Agency for Science, Technology and Research (A*STAR), Singapore 138632.

Yew-Soon Ong is with the Centre for Frontier AI Research (CFAR), Agency for Science, Technology and Research (A*STAR), Singapore, and is also with the School of Computer Science and Engineering, Data Science and Artificial Intelligence Research Centre, Nanyang Technological University (NTU).

Ke Tang is with the Guangdong Provincial Key Laboratory of Brain-Inspired Intelligent Computation, Department of Computer Science and Engineering, Southern University of Science and Technology, Shenzhen 518055, P. R. China.

In practice, misinformation, when spread explosively, has the potential to severely disrupt public order and social stability. An illustrative case took place in 2017 when the U.S. National Weather Service issued inaccurate information about the Oroville Dam evacuation. Numerous emergency calls quickly flooded the 911 dispatch center and occupied a significant portion of emergency resources for an extended time period. As a consequence of the delayed response, genuine emergency calls were left unattended during that time [3]. Another example is that a community in Uganda propagated rumors that attributed the cause of COVID-19 to evil spirits. Consequently, hate speech against foreigners surged, triggering serious social unrest in Uganda [4].

To prevent such vicious incidents, it is crucial to promptly address and contain misinformation before it spreads widely. From the problem-solving perspective, this necessitates a method capable of real-time solutions (i.e., responses within a minute) to practical IBM problems with hundreds of thousands of nodes and beyond. However, attaining this goal is non-trivial. Firstly, the IBM problem is an NP-hard combinatorial optimization problem [5], meaning that one would typically resort to approximation and heuristic algorithms, such as the greedy algorithm, to achieve low time complexity. Secondly and more importantly, assessing the blocked influence (i.e., solution quality) of an IBM problem solution is a #P-hard problem [6], which typically requires plenty of expensive Monte Carlo simulations (MCSs) for estimation (empirically 10,000 simulation replications [7]).

Unfortunately, despite the pressing needs, existing methods for solving IBM problems often fail to provide timely solutions. Budak et al. [5] conducted pioneering research on solving IBM problems and proposed an MCSs-based greedy algorithm. However, this algorithm would take approximately 16 hours to solve the IBM problems with around 6,000 nodes [8]. Subsequently, efforts have been made to reduce the number of MCSs required to solve IBM problems or to reduce the computational cost of each simulation. For example, He et al. [9] proposed to use a candidate set to reduce the search space, which identified a good solution with fewer MCSs compared to search the entire solution space. Tong and Du [10] introduced a sketch-based optimization method that avoids repetitive MCSs. Additionally, Tong [11] proposed learning a model that predicted the blocked influence of a given solution. Overall, these methods still demand a significant amount of time to solve IBM problems with thousands of nodes.

This work aims to develop a novel approach that can achieve real-time solutions to IBM problems of practical scales. Specifically, our interest lies in addressing IBM problems that

encompass hundreds of thousands of nodes and edges, with the goal of finding good solutions within seconds (less than one minute). Our key idea is to construct a fast-to-evaluate surrogate model as a substitute for the time-intensive MCSs. To this end, a learning problem is formulated to build the neural influence estimator (NIE). The NIE takes the false-and-true information instance¹ as input, extracts features describing the topology and inter-relationship between two seed sets, and predicts the blocked influence.

Such a design enables a well-trained NIE to generalize across different IBM problems with varying false-and-true information instances, on a given social network. In addition, the time complexity of NIE is remarkably low, making it highly scalable and capable of handling large-scale IBM problems effortlessly. Finally, as a solution evaluation approach, NIE can be readily combined with existing IBM optimization algorithms such as the greedy algorithm [5] and its lazy variant [12].

The main contributions are summarized as follows:

- 1) A fast influence estimator NIE is introduced to enable real-time solutions to the IBM problems of practical scales. A learning problem is formulated to obtain NIE that can predict the blocked influence of any false-and-true information instance given a social network.
- 2) A new feature extraction approach is proposed considering both the topology and the inter-relationship between the false-information seed set and the true-information seed set.
- 3) NIE is analyzed to have considerably lower time complexity than the existing influence estimators and can scale up to larger-scale networks while maintaining high efficiency.
- 4) Experimental results on 25 IBM problems with up to millions of edges verify that the NIE-based optimization method performs significantly better than the state-of-the-art methods in terms of both runtime and solution quality (given a time budget of one minute). Notably, the NIE-based optimization method can be up to four orders of magnitude faster than the MCSs-based optimization method to achieve the same solution quality. Moreover, given a real-time constraint of one minute, the NIE-based method can solve IBM problems with hundreds of thousands of nodes, which is at least one order of magnitude larger than what can be solved by existing methods.

The remainder of the paper is organized as follows. Section II reviews related works on improving the efficiency of the MCSs-based greedy algorithm. In Section III, the information diffusion model and the IBM problem are introduced. Section IV presents NIE, analyzes its time complexity, and introduces an NIE-based optimization method. Experimental results are presented in Section V, followed by the conclusion in Section VI.

¹The false-and-true information instance consists of a false-information seed set and a true-information seed set.

II. RELATED WORKS

As aforementioned, the MCSs-based greedy algorithm [5] is inefficient in tackling IBM problems. This section reviews related works on improving the efficiency of the MCSs-based greedy algorithm from two aspects: cutting the expense of a single evaluation and reducing the number of evaluations.

A. Accelerations of A Single Evaluation

The first category of acceleration methods is to limit the scope or path of influence spread. Wu and Pan [13] utilized the maximum influence arborescence structure to restrict the influence to propagate along the path with the highest propagation probability, thus reducing the simulation's time complexity. He et al. [14] picked node's local subgraph based on the directed acyclic graphs and employed a dynamic programming method to compute its influence within the subgraph. However, the limitation of these methods is their susceptibility to the graph structure, which affects the efficacy of acceleration.

The second way of reducing evaluation expenses is to avoid rerunning simulations, known as the sketch-based method. More precisely, this method pre-generates the simulation sketches and utilizes them to estimate the true influence [15]. Of the sketch-based methods, the reverse reachable sketch method (RR-Sketch) [16], [17] is proven to be efficient. RR-Sketch randomly selects a node u and generates a simulation sketch starting from u to potentially visited nodes. Then, the visited nodes form a reverse reachable set of u . Repeating this process yields a collection of reverse reachable sets, which are used to estimate the influence. Several studies have extended RR-Sketch to address IBM problems. Song et al. [18] considered an IBM problem with a deadline and exploited the weighted reverse reachable tree to calculate the probability of node u reaching root v at a specific time. The practical efficiency of the sketch-based algorithms mainly depends on the sampling strategy. Tong et al. [19] proposed a reverse-tuple based randomized algorithm which sampled the nodes more efficiently and provided an unbiased estimate for the objective. Instead of random node sampling, Tong and Du [10] developed a hybrid sampling method that assigned a higher sampling probability to the nodes that were susceptible to misinformation. This approach further enhances the optimization speed. These approaches exhibit significantly greater efficiency than MCSs for evaluations. However, their time complexity still requires improvement as they rely on obtaining a sufficient number of samples to estimate the blocked influence accurately.

In addition, machine learning techniques have been used to construct an approximate estimator for the blocked influence. Tong [11] developed a learnable scoring model, to assess the quality of different protection strategies based on the multiple subgraphs. This model was then combined with the greedy algorithm to identify the optimal protector, which is called StratLearner. Although StratLearner is faster than MCSs in influence estimation, it is still unable to provide real-time solutions. This is because the scoring model has high time complexity due to the need of calculating the weighted sum of the distance functions for all nodes in each subgraph. Unlike

Tong [11], our approach is analyzed to have much lower time complexity than StratLearner and can better address the IBM problems with real-time demands.

B. Reducing the Number of Evaluations

Both the speed and the number of evaluations can affect optimization efficiency. Some studies attempt to achieve a good solution with fewer influence estimations. Yan et al. [20] proposed a two-stage method that initially chose the candidate nodes with strong ability to block misinformation and then applied the greedy algorithm to the candidate set. He et al. [9] partitioned the network into multiple communities, selected candidate nodes from each community, and used reinforcement learning to identify high-quality solutions. Zhang et al. [21] identified the gateway nodes that enlarged the spread of misinformation to construct the candidate set and used the greedy algorithm to identify the final solution. Although reducing the number of evaluations is not the focus of this work, these techniques can be combined with our approach with ease to further enhance efficiency.

III. PROBLEM DEFINITION AND NOTATIONS

This section presents the information diffusion model of the social network and the formulation of the IBM problem.

A. Information Diffusion Model

A social network can be modeled as a directed graph $G = (V, E)$, where V denotes the set of nodes and E denotes the set of connections between each pair of nodes. Suppose there are two types of information spreading in the social network: false information and true information. Each node in the network is assigned one of three states: F -active (activated by the false information), T -active (activated by the true information), or Θ -active (inactive).

This work considers the widely used independent cascade model to simulate the influence diffusion process in IBM [10]. Correspondingly, there are two cascades: C_f for false information and C_t for true information. Each edge $(u, v) \in E$ is assigned a propagation probability $\Pr[(u, v)] \in (0, 1]$ to indicate the probability that node u activates node v . Let S_f and S_t denote the false-information seed set and the true-information seed set, respectively. At step $t = 0$, the diffusion of two cascades starts from S_t and S_f . At step $t = T (T > 0)$, the F -active (or T -active) node u has one chance to activate its neighbor Θ -active node v with the probability $\Pr[(u, v)]$. When there are an F -active node u_f and a T -active node u_t trying to trigger their shared neighbor Θ -active node v simultaneously, the priority is given to u_f .² Once a node is activated, its state becomes fixed, and the information continues to propagate until the states of all the node remain unchanged. Given G , S_t , and S_f , the final number of F -active nodes is a random variable due to the inherent uncertainty of the information diffusion process.

²Our method can also be applied to the case where true information has priority with minor adjustments.

B. The IBM Problem

Prior to introducing the IBM problem, we define non-misinformation influence and blocked influence below.

Definition 1: (Non-misinformation Influence) Let \bar{F} -active represent the state that is not F -active, i.e., T -active or Θ -active. Given a social network G , a false-information seed set S_f , and a true-information seed set S , the non-misinformation influence $g(S|S_f)$ is defined as the expected number of \bar{F} -active nodes. That is, $g(S|S_f) = E[G(S, \omega|S_f)]$ where the random variable $G(S, \omega|S_f)$ denotes the number of \bar{F} -active nodes, and ω denotes the random noise representing the uncertainty regarding nodes being activated or not.

Definition 2: (Blocked Influence) The blocked influence $f(S_t|S_f)$ is defined as the difference between the non-misinformation influence with $S = S_t$ and the non-misinformation influence with $S = \emptyset$, i.e., $f(S_t|S_f) = g(S_t|S_f) - g(\emptyset|S_f)$.

Given a social network G and a false-information seed set S_f , the IBM problem is to select a true-information seed set S_t such that the blocked influence $f(S_t|S_f)$ is maximized with the constraint on the size of S_t . Formally, the IBM problem is formulated as follows.

$$\begin{aligned} \max_{S_t \subset V \setminus S_f} \quad & f(S_t|S_f) = g(S_t|S_f) - g(\emptyset|S_f) \\ \text{s.t.} \quad & |S_t| \leq K, \end{aligned} \quad (1)$$

where $K \in \mathbb{Z}^+$ is the maximum size of S_t .

C. MCSs-based Estimator

In Problem (1), $g(S|S_f)$ has no analytical form and can be estimated by Monte Carlo simulations (MCSs). The time complexity of MCSs is $\mathcal{O}(rm)$ where r denotes the number of simulation replications and m denotes the number of edges [15]. The challenge in estimating $g(S|S_f)$ using MCSs is the high computational burden, which can be viewed from two aspects. Firstly, in one simulation, there is at most one chance to determine whether u will activate v for $\forall (u, v) \in E$. Therefore, the worst-case time complexity for one simulation is $\mathcal{O}(m)$. Practical social networks often consist of more than hundreds of thousands of edges, which significantly increases the time required to execute a single simulation. Secondly, let $G(S, \omega_i|S_f)$ be the i -th simulation sample of the number of \bar{F} -active nodes given random noise ω_i . Then $g(S|S_f)$ can be estimated by the sample mean $\bar{G}(S|S_f) = \sum_{i=1}^r G(S, \omega_i|S_f)/r$. Here, we make the mild assumptions that $E[G(S, \omega|S_f)] < \infty$ for $\forall S \subset V \setminus S_f$ and $G(S, \omega_i|S_f) (i = 1, \dots, r)$ are independent and identically distributed, which commonly hold in the simulation studies [22]–[26]. According to the strong law of large numbers, the accurate estimation of $g(S|S_f)$ requires plenty of simulation replications, e.g., $r = 10,000$ [7].

IV. NEURAL INFLUENCE ESTIMATOR

Our goal is to learn a fast approximation of MCSs, thus accelerating the optimization of IBM problems. Specifically, we seek to build a neural influence estimator (NIE) that can 1) generalize well across different IBM problems with varying false-information seed sets, and 2) possess exceptionally low

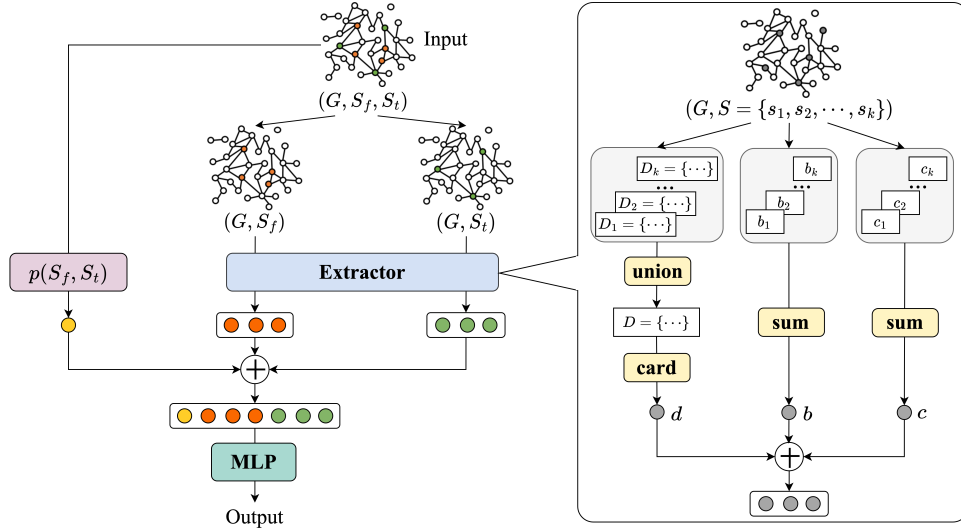


Fig. 1. The architecture of NIE.

time complexity such that it can scale up to social networks involving hundreds of thousands of nodes and edges.

This section firstly formulates the learning problem and describes the structure of NIE. Then, the time complexity of NIE is analyzed and compared with that of existing methods, followed by an NIE-based optimization method.

A. The Learning Problem

In reality, social networks like Weibo and Twitter exhibit relatively stable structures, while the sources of false information tend to vary. For example, for different types of rumors, the choices of seed nodes can be different. With this in mind, we seek to construct a surrogate model that can predict the blocked influence for any false-and-true information instance on a given social network G . Here, a false-and-true information instance \mathbf{I} refers to a pair of false-information seed set S_f and true-information seed set S_t , i.e., $\mathbf{I} = (S_f, S_t)$. Let $\hat{f}(\mathbf{I})$ be the predicted blocked influence of \mathbf{I} and $f_{MCSs}(\mathbf{I})$ be the corresponding blocked influence estimated by MCSs. Then, the loss function based on the mean squared error (MSE) is $Loss = (1/T) \sum_{t=1}^T [\hat{f}(\mathbf{I}_t) - f_{MCSs}(\mathbf{I}_t)]^2$ where T is the size of training data.

B. NIE Architecture

Neural networks have shown outstanding capabilities in modeling the nonlinear relationship between input and output, making them extensively utilized as surrogate models for computationally expensive modules [27], [28]. To maintain low computational complexity, we opt for the multilayer perceptron (MLP) as the regression model because of its inherent simplicity. However, learning the mapping from the false-and-true instance \mathbf{I} to the blocked influence is a challenging task due to the intricate topology and inter-relationship of S_f and S_t . To tackle this challenge, we propose to extract informative graph features from \mathbf{I} , thereby rendering the subsequent prediction task tractable. Figure 1 illustrates the architecture of NIE.

1) *Input of NIE*: The input of NIE includes a graph G and a false-and-true information instance \mathbf{I} . Extracting comprehensive useful features from the raw input data (G, \mathbf{I}) poses two challenges.

- The nodes in S_f (or S_t) have tight connectivity with the rest of nodes in G . Q1 : How to adequately extract topological patterns of S_f (or S_t) in the whole graph?
- The connectivity of S_f and S_t greatly affects the blocked influence. Q2 : How to quantify the inter-relationship of the two sets in the graph?

2) *Feature Extraction*: As shown in Figure 1, the features are extracted considering the topology and inter-relationship of S_f and S_t . Initially, the input data (G, S_f, S_t) is divided into (G, S_f) and (G, S_t) , allowing for the extraction of topological features from (G, S_f) and (G, S_t) independently. Next, a feature $p(S_f, S_t)$ is computed to capture the inter-relationship between S_f and S_t . Lastly, these features are concatenated as the input of the subsequent predictor.

The topological patterns of S_f and S_t are extracted from (G, S_f) and (G, S_t) , respectively, focusing on the aspects of neighborhood, location, and structure.

- **Neighborhood**: The neighborhood feature is characterized by the size of the neighbor nodes of set $S = \{s_1, s_2, \dots, s_k\}$. We gather the set D_i that comprises the neighbor nodes for each $s_i \in S$ and obtain the union set $D = \bigcup_{i=1}^k D_i$. The neighborhood feature d is defined as the size of D .
- **Location**: The location feature reflects how central S is in graph G or how close S is to the rest nodes in G . Correspondingly, the location feature $b = \sum_{i=1}^{|S|} b_i$ where $b_i = L / \sum_{l=1}^L d(s_i, v_l)$ is the closeness centrality of node $s_i \in S$, L is the number of nodes reachable from s_i , and $d(s_i, v_l)$ is the shortest-path distance from s_i to v_l [29].
- **Structure**: The structure feature refers to the border structure of S and is defined as the degree to which the neighbor nodes of S gather into clusters. Specifically, the structure feature c is the sum of all the clustering

Algorithm 1: Approximation of $\Pr\{s_i \text{ is } F\text{-active}|S_f\}$ for $\forall s_i \in S_f^H$

Input: S_f^H, H .**Output:** $\Pr\{s_i \text{ is } F\text{-active}|S_f\}$ for $\forall s_i \in S_f^H$.

- 1 Set the counter $h \leftarrow 1$, and let V_s denote the set of the parent nodes of s ;
 - 2 **for** $\forall s_i \in S_f^H$ **do** calculate the propagation coefficient $pc_{s_i} \leftarrow \sum_{u \in V_{s_i}} \Pr[(u, s_i)]/|V_{s_i}|$;
 - 3 **for** $\forall s_i \in S_f^1$ **do** $\Pr\{s_i \text{ is } F\text{-active}|S_f\} \leftarrow pc_{s_i}$;
 - 4 **while** $h \leq H - 1$ **do**
 - 5 $h \leftarrow h + 1$;
 - 6 **for** $\forall s_i \in S_f^h \setminus S_f^{h-1}$ **do** $\Pr\{s_i \text{ is } F\text{-active}|S_f\} \leftarrow pc_{s_i} \cdot \left\{1 - \prod_{s_j \in S_f^{h-1} \cap V_{s_i}} [1 - \Pr\{s_j \text{ is } F\text{-active}|S_f\}]\right\}$;
 - 7 **end**
-

coefficient c_i for $s_i \in S$. Here $c_i = T(s_i)/\{2deg^{tot}(s_i) \cdot [deg^{tot}(s_i) - 1] - 2deg^{\leftrightarrow}(s_i)\}$ for $s_i \in S$, where $T(s_i)$ is the number of directed triangles through node s_i , $deg^{tot}(s_i)$ is the sum of in-degree and out-degree of s_i , and $deg^{\leftrightarrow}(s_i)$ denotes the reciprocal degree of s_i [29].

The inter-relationship between S_f and S_t is described by the protective ability of S_t to the nodes around S_f , which can be quantified by $p(S_f, S_t)$:

$$p(S_f, S_t) = \sum_{s_i \in S_f^H} [\Pr\{s_i \text{ is } F\text{-active}|S_f\} \cdot \mathbb{1}\{d(S_t, s_i) < d(S_f, s_i)\}], \quad (2)$$

where S_f^H denotes the set of nodes to which the shortest distance from S_f is less than or equal to H -hops. Here, the shortest distance from a node set S to a node s_i , denoted as $d(S, s_i)$, is $\min_{u \in S} d(u, s_i)$, where $d(u, s_i)$ is the shortest distance in terms of hops from u to s_i in graph G .

Specifically, $p(S_f, S_t)$ involves two components: the weight function $\Pr\{s_i \text{ is } F\text{-active}|S_f\}$ and the judgment function $\mathbb{1}\{d(S_t, s_i) < d(S_f, s_i)\}$. The weight function measures the probability that s_i is activated by the false information without considering S_t . A higher probability means that the node requires more attention and protection. The judgment function evaluates the effectiveness of S_t in safeguarding s_i , considering both S_f and S_t . A greater value of $p(S_f, S_t)$ indicates a stronger ability of S_t to safeguard the neighbor nodes of S_f .

In Eq. (2), it is intractable to accurately calculate $\Pr\{s_i \text{ is } F\text{-active}|S_f\}$ due to its dependence on the uncertain states of the neighbors of s_i . To address this issue, we propose to approximate $\Pr\{s_i \text{ is } F\text{-active}|S_f\}$, as described in Algorithm 1. Intuitively, a node s_i is F -active when there exists at least one F -active parent node of s_i and the false information can propagate to s_i . Algorithm 1 first calculates the propagation coefficient pc_{s_i} for each node in S_f^H (line 2). Then, for $\forall s_i \in S_f^1$, pc_{s_i} is directly used to approximate $\Pr\{s_i \text{ is } F\text{-active}|S_f\}$ (line 3); while for $\forall s_i \in S_f^h \setminus S_f^{h-1}$ ($2 \leq h \leq H$), $\Pr\{s_i \text{ is } F\text{-active}|S_f\}$ is determined by the product of the propagation coefficient and the probability that there exists at least one parent node being F -active (lines 4-7).

3) *MLP Layer:* The extracted features are fed into MLP, and the output is the predicted blocked influence $\hat{f}(I)$. For MLP, the hidden layers are fully connected followed by a rectified linear unit (ReLU) activation function. Early stopping is used to prevent overfitting.

C. Complexity Analysis and Comparison

This section analyzes the time complexity of NIE and compares it with other influence estimators. For brevity, we denote $n = |V|$, $m = |E|$, $k_f = |S_f|$, and $k_t = |S_t|$.

1) *Complexity Analysis for NIE:* The main components in NIE consist of the Extractor, $p(S_f, S_t)$, and MLP. Among them, the time complexity of MLP is independent of network scale (i.e., number of nodes and edges). In practice, the computational time of MLP is almost negligible, compared to the computational time of the other two components. Hence, we analyze the time complexities of the Extractor and $p(S_f, S_t)$.

The time complexity of the Extractor is determined by the **union** operation. The time complexities of the Extractor for (G, S_f) and the Extractor for (G, S_t) are $\mathcal{O}(k_f \cdot \min(m, n))$ and $\mathcal{O}(k_t \cdot \min(m, n))$ respectively, because the Hash table can be used to obtain D and the number of nodes connected to S_f (or S_t) is bounded by m and n . Hence, the overall time complexity of the Extractor is $\mathcal{O}((k_f + k_t) \cdot \min(m, n))$.

To compute $p(S_f, S_t)$ in Eq. (2), we firstly construct set S_f^H . Let $S_f^H = \emptyset$. The seed nodes in S_f are sequentially chosen as the initial point x_0 to spread the influence. The breadth-first search is performed to visit the node s_i whose distance to x_0 is less than or equal to H . If $s_i \notin S_f^H$, add s_i into S_f^H . The above process is repeated until all solutions in S_f are traversed. The size of S_f^H is bounded by m and n . Therefore, the worst-case time complexity for constructing S_f^H is $\mathcal{O}(\min(m, n))$. Secondly, for $\forall s_i \in S_f^H$, $d(S_f, s_i)$ and $d(S_t, s_i)$ are selected by the BFPRT algorithm [30]. Their worst-case time complexities are $\mathcal{O}(k_f \cdot \min(m, n))$ and $\mathcal{O}(k_t \cdot \min(m, n))$, respectively, because $|S_f^H|$ is bounded by m and n and the worst-case time complexity for selecting $d(S_f, s_i)$ (or $d(S_t, s_i)$) is $\mathcal{O}(k_f)$ (or $\mathcal{O}(k_t)$). Lastly, the $\Pr\{s_i \text{ is } F\text{-active}|S_f\}$ is computed for $\forall s_i \in S_f^H$. As shown in Algorithm 1, the false information propagates from the nodes in layer $h-1$ to the nodes in layer h ($h = 2, \dots, H$). If there exists an edge from s_j ($s_j \in S_f^{h-1}$) to s_i ($s_i \in S_f^h$), $1 - \Pr\{s_j \text{ is } F\text{-active}|S_f\}$ is calculated in Step 5. The number of calculations is bounded by m and

TABLE I
COMPARISON IN TERMS OF TIME COMPLEXITIES OF DIFFERENT INFLUENCE ESTIMATORS.

Estimator	Time Complexity	Explanation
NIE	$\mathcal{O}((k_f + k_t) \cdot \min(m, n))$	n, m, k_f, k_t are the node number, edge number, size of the false-information seed set S_f , and size of the true-information seed set S_t , respectively.
MCSs	$\mathcal{O}(r \cdot m)$	r is the number of simulation replications.
HMP*	$\mathcal{O}(l \cdot k_t \cdot \min(m, n))$	l is the number of R -samples.
StratLearner*	$\mathcal{O}(t \cdot (k_f + k_t) \cdot n)$	t is the number of subgraphs.

n because the number of the edges between all the adjacent layers is less than or equal to m and $|S_f^H|$ is bounded by m and n . Therefore, the worst-case time complexity of Algorithm 1 is $\mathcal{O}(\min(m, n))$. Consequently, the worst-case time complexity of computing $p(S_f, S_t)$ is $\mathcal{O}((k_f + k_t) \cdot \min(m, n))$. Combining the complexity of the Extractor, the overall complexity of NIE is $\mathcal{O}((k_f + k_t) \cdot \min(m, n))$.

2) *Complexity Comparison of Different Influence Estimators*: We compare NIE with three existing influence estimators used by the state-of-the-art IBM methods. **MCSs** is the baseline approach to estimating the blocked influence. **HMP*** represents the estimator used by the sketch-based method HMP [10]. **StratLearner*** is a learning-based surrogate model that estimates influence in the method StratLearner [11]. Table I presents the time complexities of these estimators. For detailed complexity analyses for HMP* and StratLearner*, please refer to the Appendix.

For MCSs, the number of simulation replications r should be large enough, empirically $r = 10,000$ [7]. For StratLearner*, it is recommended that the number of subgraphs t should be at least 400 for accurate estimations [11]. For HMP*, l is the number of R -samples, which should be set sufficiently large as recommended in [10]. In practice, it holds that $k_t + k_f \ll r$ and $k_t + k_f \ll l$. Hence, the time complexity of NIE is much lower than that of MCSs, HMP*, and StratLearner*.

D. NIE-based Optimization Method

The surrogate model NIE can be integrated into any MCSs-based optimization method for solving IBM problems. In this work, we integrate NIE into the cost-effective lazy forward selection algorithm (CELF) [12], an advanced variant of the greedy algorithm. The resultant method, called NIE-CELF, is illustrated in Algorithm 2. It is worth mentioning that NIE-CELF can be further combined with heuristics such as [20],

Algorithm 2: NIE-CELF

Input: K, S_f, G

Output: S_t

- 1 Set the counter $k \leftarrow 0$ and $S_t \leftarrow \emptyset$;
 - 2 **while** $k \leq K - 1$ **do**
 - 3 $k \leftarrow k + 1$;
 - 4 $v^* \leftarrow \text{LazyForward}(\hat{f}(\mathbf{I}), S_f, S_t, G)$ [12];
 - 5 $S_t \leftarrow S_t \cup \{v^*\}$.
 - 6 **end**
-

TABLE II
NETWORK STATISTICS.

Network	# Nodes	# Edges	Average Degree
power-law graph	768	1,532	1.99
email-Eu-core	1,005	25,571	25.44
p2p-Gnutella08	6,301	20,777	3.30
p2p-Gnutella24	26,518	65,369	2.47
web-Stanford	281,903	2,312,497	8.20

[21] to reduce the number of evaluations and achieve even higher efficiency.

V. EXPERIMENTAL STUDIES

The experiments aim to assess the efficiency and scalability of NIE. To this end, we select five social networks with varying scales, generate 25 IBM problems, and compare NIE-CELF with four state-of-the-art methods. Specifically, two sets of experiments are conducted. In the first experiment, the performance of different methods is compared in terms of the runtime required to achieve a predefined solution quality. In the second experiment, the methods are compared from the perspective of solution quality obtained using a time budget. In addition, the feature importance of NIE, as well as the settings of H and the hyperparameters of MLP, are also discussed.

A. Experimental Setup

1) *Networks and Test Problems*: Five networks [8], [11] with different scales, structures, and average degrees are considered in the experiments. Table II summarizes their statistics. **Power-law graph** simulates the common power-law distributed network. **Email-Eu-core** is built based on the email data from a large European research institution to describe the email network across 42 different departments. **P2p-Gnutella08** and **p2p-Gnutella24** are established based on the snapshot data from the Gnutella peer-to-peer file sharing network to describe the connections between different hosts in the network. **Web-Stanford**, sourced from the Stanford University website, describes the hyperlink relationship between different pages.

Based on each network, we generate five IBM problems, meaning there are 25 test problems in total. Specifically, each problem is generated in the following way. First we rank all the nodes according to their out-degrees, add the top ρ nodes into a high-impact set V^* , and then randomly select S_f from V^* , i.e., each S_f corresponds to a test problem. The

TABLE III
PARAMETER SETTINGS FOR THE COMPARED METHODS.

Method	Parameter Description	Value
MCSs-CELF	Simulation replications (r)	10,000
HMP*-CELF	Number of R -sampled (l)	10,000
StratLearner*-CELF	Training set size	192
	Number of subgraphs (t)	400
CMIA-O	Influence threshold	0.01

size of S_f is sampled from a power-law distribution with the shape parameter 9 and the scale parameter 10. The above selection rule for S_f is reasonable in practice because the false information typically targets nodes with high impact to achieve wider dissemination. We set $\rho = 1\%$ for the web-Stanford network and $\rho = 10\%$ for other networks. For each test problems, the maximum size of S_t , i.e., K in Problem (1), equals to $|S_f|$. For the information diffusion model (see Section III-A), we adopt the commonly used propagation probability $P[(u, v)] = 1/d(v)$ where $d(v)$ is the in-degree of node v [5], [10], [13].

2) *Compared Methods*: NIE-CELF are compared with four state-of-the-art methods: MCSs-CELF, HMP*-CELF, StratLearner*-CELF, and CMIA-O. The first three methods combine the influence estimators MCSs, HMP*, and StratLearner* (see Table I) with the same optimization algorithm CELF. Note that in the original publications of HMP [10] and StratLearner [11], these methods are implemented using the greedy algorithm. Compared to the greedy algorithm, CELF achieves much higher efficiency without compromising solution quality, thus in the experiments we replace the greedy algorithm with CELF for these methods. Finally, CMIA-O [13] is a heuristic method for solving IBM problems that limits the influence propagation path to enhance efficiency. Experimental results in [13] show that CMIA-O is much faster than the MCSs-based greedy algorithm.

3) *Performance Metrics*: The concerned performance metrics are optimization speed and solution quality. We measure the former with the runtime of the optimization method, denoted as T . For the latter, we measure it with $\hat{f}_{MCSs}(\hat{S}_t^*|S_f)$, which is the blocked influence estimated by MCSs with S_t^* being the solution found by the optimization method.

4) *Experimental Protocol*: The parameters of the compared methods are set as recommended in the literature and are summarized in Table III. For NIE-CELF, we conduct preliminary experiments to determine H and the hyperparameters of MLP (see Section V-E). Specifically, H is set to 3 for the web-Stanford network and 2 for other networks. For MLP, two hidden layers are applied and the dimension of each hidden layer is 128; batch size and learning rate are set to 512 and 0.05, respectively. To train NIE, for each network, we generate 100,000 training examples. Each example contains a false-and-true information instance $\mathbf{I} = (S_f, S_t)$ and its corresponding blocked influence estimated by 1,000 replications of MCSs. Here, S_f is randomly selected as previously described and S_t is randomly selected from $V \setminus S_f$ with $|S_t| = |S_f|$.

Since MCSs-CELF and HMP*-CELF contain stochastic components, their results are obtained by executing the method

for 5 independent runs. For all the compared methods, T and $\hat{f}_{MCSs}(\hat{S}_t^*|S_f)$ in each iteration are recorded. The termination condition is either reaching the maximal number of iterations, or exceeding the runtime limit of 48 hours. To make a fair comparison, all methods are implemented in Python and run on the same computing platform, i.e., Intel Xeon Gold 6336Y CPU with 3.6G Hz and 256GB of memory.

B. Comparison in Terms of Runtime

In this work, the most concerned performance indicator is the runtime T . This section compares the runtime of different methods given a target solution quality. The target quality is determined by the final objective value achieved by NIE-CELF. Since it is challenging to ensure that two methods achieve the exactly same objective value during the optimization process, we adopt the following comparison approach that is slightly unfair to NIE-CELF. That is, the compared method is considered to have reached the target quality if it, for the first time, discovers a solution whose quality is not worse than the target quality, and then the recorded runtime of its previous iteration is reported. If the compared method fails to find such a solution, the runtime at which the method terminates is reported.

Table IV lists the runtime of the methods to achieve the target solution quality. The first observation from Table IV is that NIE-CELF can solve the test problems mostly within one second. For the web-Stanford network with more than 280,000 nodes and 2,300,000 edges, NIE-CELF can solve the test problems within 30 seconds. These results demonstrate that NIE-CELF can achieve real-time solutions to IBM problems of practical scales. Moreover, it can be observed that all the compared methods consume much more runtime than NIE-CELF on all the test problems, except on the second problem of the power-law graph network where NIE-CELF consumes slightly more runtime than CMIA-O. In fact, some methods such as MCSs-CELF and StratLearner*-CELF even fail to reach the target solution quality in 48 hours on the test problems with more than 10,000 nodes. On each network, the average ratio between the runtime of the compared method and that of NIE-CELF, i.e., average speedup, is also presented in Table IV. Notably, on all the five networks, NIE-CELF achieves substantial speedups over all the compared methods. For example, compared with MCSs-CELF, NIE-CELF is at least four orders of magnitude faster on the test problems with more than 1,000 nodes.

Furthermore, we utilize the Mann-Whitney U test with a significance level $\alpha = 0.05$ to determine whether there is a significant difference between the average runtime of NIE-CELF and that of the compared method on the same network. The comparison results show that NIE-CELF is significantly better than all the compared methods on all the networks, except on the smallest network power-law graph the difference between NIE-CELF and CMIA-O is not significant. Nevertheless, NIE-CELF can scale up to large-scale networks much better than CMIA-O, since the runtime of the latter increases dramatically with the problem scale. Overall, these observations clearly demonstrate the superiority of NIE-CELF

TABLE IV
THE RUNTIME (IN SECONDS) REQUIRED BY THE METHODS TO ACHIEVE THE TARGET SOLUTION QUALITY. THE LOWER, THE BETTER.

Network	V	E	Problem	Method				
				NIE-CELF	MCSs-CELF	HMP*-CELF	StratLearner*-CELF	CMIA-O
power-law graph	768	1,532	1	0.27	184.18	7.49	117.35	0.36
			2	0.41	117.23	6.77	101.69	0.39
			3	0.19	128.48	4.47	65.02	0.26
			4	0.18	232.55	14.59	193.08	1.29
			5	0.23	294.01	16.87	274.50	1.33
Average speedup Comparison result					842.91 w	44.44 w	658.20 w	3.32 d
email-Eu-core	1,005	25,571	1	0.78	9943.50	51.27	166.74	<u>86.43</u>
			2	0.60	16092.73	50.74	253.14	<u>77.16</u>
			3	1.06	3576.73	36.25	189.28	<u>93.67</u>
			4	0.72	4839.09	33.82	192.95	<u>109.01</u>
			5	0.65	6458.17	36.34	163.83	<u>91.35</u>
Average speedup Comparison result					11920.03 w	57.48 w	266.85 w	123.94 w
p2p-Gnutella08	6,301	20,777	1	0.31	8370.16	175.69	<u>172800.00</u>	<u>158.81</u>
			2	0.25	2629.84	132.94	<u>172800.00</u>	<u>112.22</u>
			3	0.25	5815.10	194.24	<u>172800.00</u>	<u>234.29</u>
			4	0.24	7308.41	185.82	<u>172800.00</u>	<u>169.95</u>
			5	0.26	3178.32	82.34	<u>172800.00</u>	<u>43.81</u>
Average speedup Comparison result					20691.26 w	593.28 w	664886.95 w	554.99 w
p2p-Gnutella24	26,518	65,369	1	0.72	<u>172800.00</u>	220.60	<u>172800.00</u>	<u>44.47</u>
			2	0.65	<u>172800.00</u>	746.72	<u>172800.00</u>	<u>237.38</u>
			3	0.64	<u>172800.00</u>	473.68	<u>172800.00</u>	<u>104.56</u>
			4	0.66	<u>172800.00</u>	346.81	<u>172800.00</u>	<u>72.45</u>
			5	0.65	<u>172800.00</u>	367.80	<u>172800.00</u>	<u>209.82</u>
Average speedup Comparison result					260702.10 w	657.33 w	260702.10 w	204.58 w
web-Stanford	281,903	2,312,497	1	26.11	<u>172800.00</u>	95.27	<u>172800.00</u>	<u>127014.48</u>
			2	29.69	<u>172800.00</u>	253.54	<u>172800.00</u>	<u>128309.73</u>
			3	23.03	<u>172800.00</u>	108.13	<u>172800.00</u>	<u>5091.59</u>
			4	26.27	<u>172800.00</u>	218.33	<u>172800.00</u>	<u>95039.35</u>
			5	21.08	<u>172800.00</u>	108.58	<u>172800.00</u>	<u>7540.60</u>
Average speedup Comparison result					6943.35 w	6.07 w	6943.35 w	2676.57 w

^a For each test problem, the best runtime is indicated in bold.

^b The underline “” means that the method fails to reach the target solution quality when it is terminated due to either reaching the maximum iterations or using up the time budget of 48 hours.

^c “Average speedup” indicates the average runtime ratio between the compared method and NIE-CELF across all the five test problems on the network.

^d “Comparison result” indicates the result of the Mann-Whitney U test with a significance level of 0.05. “w” (or “l”) means that the runtime of NIE-CELF is significantly better (or worse) than that of the compared method. “d” means that the runtime difference is not significant.

to the compared methods, in terms of obtaining real-time solutions to large-scale IBM problems.

C. Comparison in Terms of Solution Quality

In addition to runtime, the other important performance metric is the solution quality that can be achieved within a time budget. Since this work focuses on real-time solutions, each method is given a time budget of one minute.

Table V presents the solution quality achieved by the methods. The first observation from these results is that NIE-CELF is the only method that can obtain solutions for all the test problems. In contrast, the compared methods fail to find real-time solutions for large-scale test problems. Similar to the previous experiments, we utilize the Mann-Whitney U test with a significance level $\alpha = 0.05$ to determine whether there

is a significant difference between the solution quality of NIE-CELF and that of the compared method on the same network (note that the test is only conducted when the compared method has available results). The comparison results show that although on some small-scale networks the compared methods can achieve better solution quality, the quality difference between them and NIE-CELF is not significant.

Furthermore, the performance of the methods is also tested using a much longer time budget of 48 hours. Figure 2 plots the solution quality of these methods along runtime (in log domain). For the sake of brevity, for each network, only the results on one problem are illustrated. Compared to other methods, NIE-CELF exhibits a significant advantage in terms of efficiency. It can find high-quality solutions much faster than others, often by several orders of magnitude, though its final solution quality might be lower than that of the other

TABLE V
THE SOLUTION QUALITY (OBJECTIVE VALUE) ACHIEVED BY THE METHODS WITH A TIME BUDGET OF ONE MINUTE. THE HIGHER, THE BETTER.

Network	V	E	Problem	Method				
				NIE-CELF	MCSs-CELF	HMP*-CELF	StratLearner*-CELF	CMIA-O
power-law graph	768	1,532	1	44.39	-	56.34	-	53.83
			2	51.85	-	75.33	-	73.69
			3	40.75	28.19	45.02	-	44.31
			4	74.83	-	106.98	-	96.84
			5	84.65	-	107.48	-	95.00
Comparison result					-	d	-	d
email-Eu-core	1,005	25,571	1	51.67	-	49.71	-	-
			2	55.50	-	55.72	-	-
			3	38.89	-	49.43	-	-
			4	38.05	-	52.60	-	-
			5	41.05	-	49.29	-	-
Comparison result					-	d	-	-
p2p-Gnutella08	6,301	20,777	1	210.37	-	-	-	-
			2	107.26	-	-	-	-
			3	352.04	-	-	-	-
			4	300.95	-	-	-	-
			5	86.34	-	-	-	63.01
Comparison result					-	-	-	-
p2p-Gnutella24	26,518	65,369	1	123.02	-	-	-	47.55
			2	385.96	-	-	-	-
			3	340.15	-	-	-	92.59
			4	285.00	-	-	-	196.06
			5	323.32	-	-	-	-
Comparison result					-	-	-	-
web-Stanford	281,903	2,312,497	1	122.82	-	-	-	-
			2	183.60	-	-	-	-
			3	112.22	-	-	-	-
			4	229.60	-	-	-	-
			5	82.06	-	-	-	-
Comparison result					-	-	-	-

^a For each test problem, the best solution quality is indicated in bold.

^b “-” means that the method fails to find a solution with a time budget of one minute.

^c “Comparison result” indicates the result of the Mann-Whitney U test with a significance level of 0.05. “w” (or “l”) means that the solution quality of NIE-CELF is significantly better (or worse) than that of the compared method. “d” means that the quality difference is not significant.

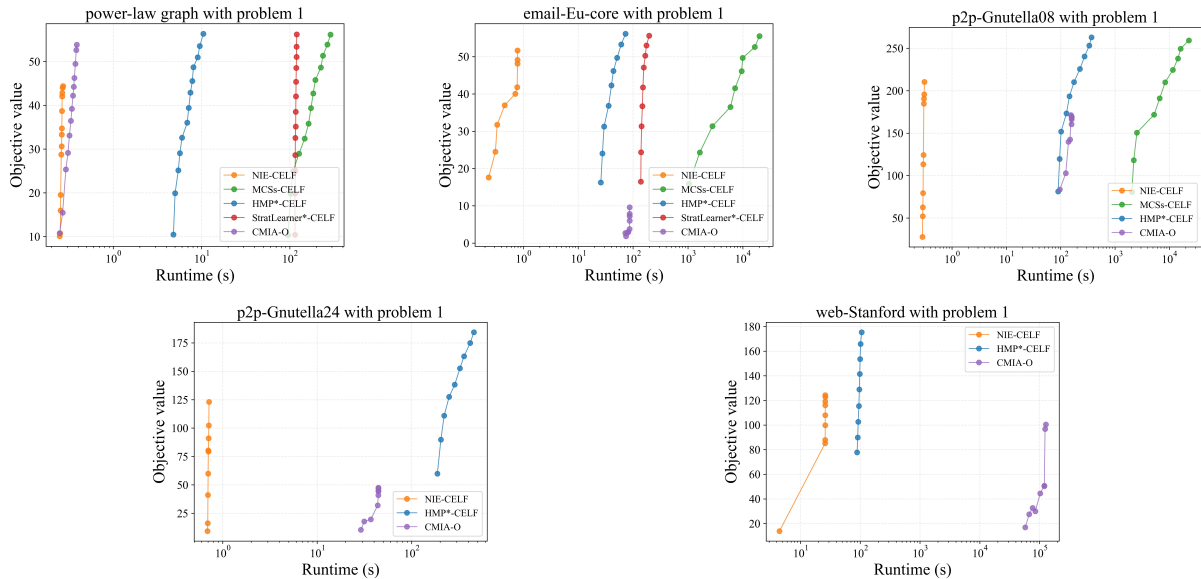


Fig. 2. Curves of the objective value vs. runtime of the optimization methods on five test problems, within a time budget of 48 hours.

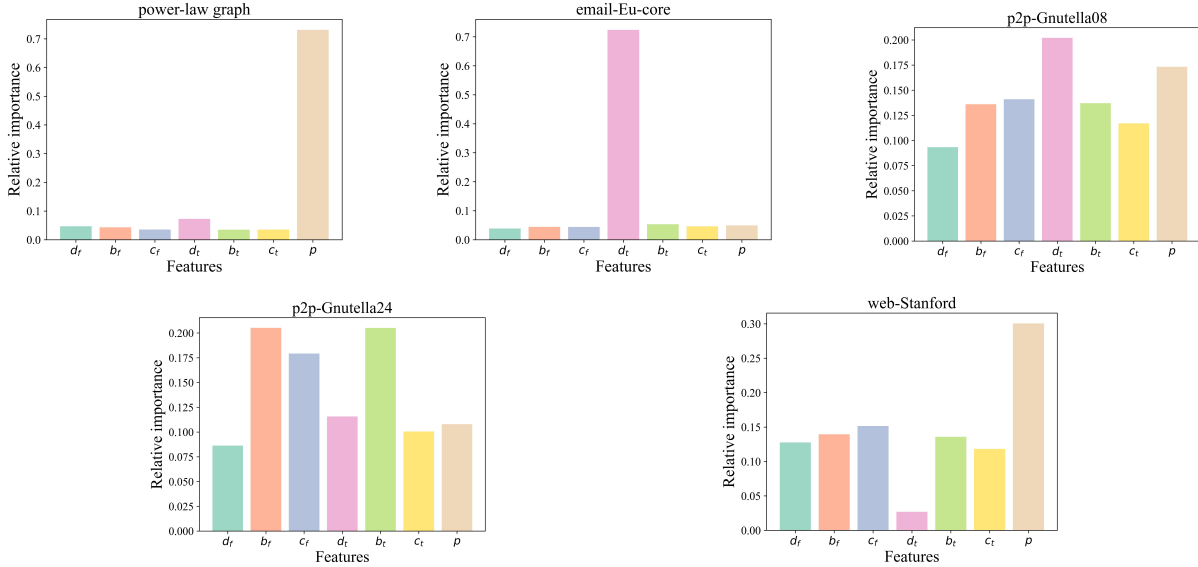


Fig. 3. Feature importance analysis for NIE.

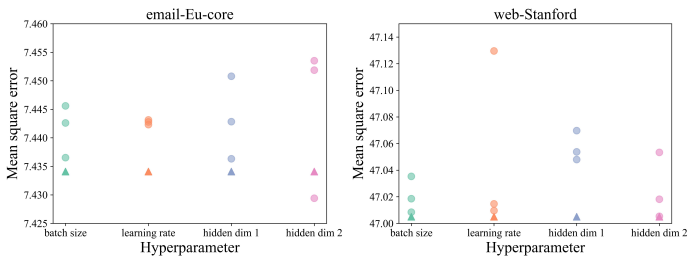


Fig. 4. Performance of MLP under different hyperparameters values. The triangle represents the MSE of the baseline configuration, and circles represent the MSE of the modified configurations.

methods. This strongly indicates the suitability of NIE-CELF for scenarios where a high-quality solution to IBM problems needs to be obtained promptly.

D. Feature Importance Analysis

This section investigates the contributions of different features to NIE. The relative importance score of each feature is obtained using the CART method [31]. Figure 3 illustrates the feature importance on all the networks. It can be observed that the importance of features varies significantly across different networks. For example, for p2p-Gnutella08 and p2p-Gnutella24, the seven features have similar importance, while for power-law graph and email-Eu-core, the inter-relationship feature p and the location feature of S_t (i.e., d_t) have significantly higher importance than other features, respectively. Overall, all the features hold importance, and it is recommended to employ all the features when building NIE for a new network.

E. Choices of H and Hyperparameters of MLP

This section discusses how to set H and the hyperparameters of MLP. For the sake of brevity, we show the results on the

email-Eu-core and web-Stanford which represent small-scale and large-scale networks, respectively.

As shown in Section IV-C, larger H can capture more graph information but requires more runtime. Practically, H does not need to be too large because the well-known small world phenomenon reveals that two nodes are linked by short chains in the social network [32]. Therefore, we test $H \in \{2, 3\}$ for web-Stanford and $H \in \{2, 3, 4\}$ for email-Eu-core. Figure 5 confirms this observation and shows that larger H leads to a better objective value but consumes more runtime. To balance runtime and solution quality, we choose $H = 3$ for web-Stanford and $H = 2$ for other networks.

To set the hyperparameters of MLP, we start from a baseline hyperparameter configuration: batch size 512, learning rate 0.05, and a dimension of 128 for each hidden layer. Then we vary one hyperparameter each time and record the MSE on an independent validation set. Specifically, hyperparameter values in a wide range are tested: batch size $\in \{128, 256, 512, 1048\}$, learning rate $\in \{0.001, 0.005, 0.01, 0.05\}$, dimension of the first hidden layer $\in \{64, 128, 256, 512\}$, dimension of the second hidden layer dimension $\in \{64, 128, 256, 512\}$. Figure 4 displays the MSE under different hyperparameter configurations. We find that the relative changes of MSE between the baseline configuration and the modified configurations are all less than 0.3%. Thus, MLP hyperparameters have minimal impact on its performance, allowing for consistent hyperparameter values across different networks.

VI. CONCLUSION

This work focuses on achieving real-time solutions to IBM problems, which is crucial in practice. A surrogate model, called NIE, is proposed as a fast approximation of the time-consuming MCSs. NIE is shown to generalize across different IBM problems with varying false-and-true information instances on a given network. Moreover, NIE has exceptionally low time complexity, making it highly scalable and capable of efficiently handling large networks with hundreds of thousands

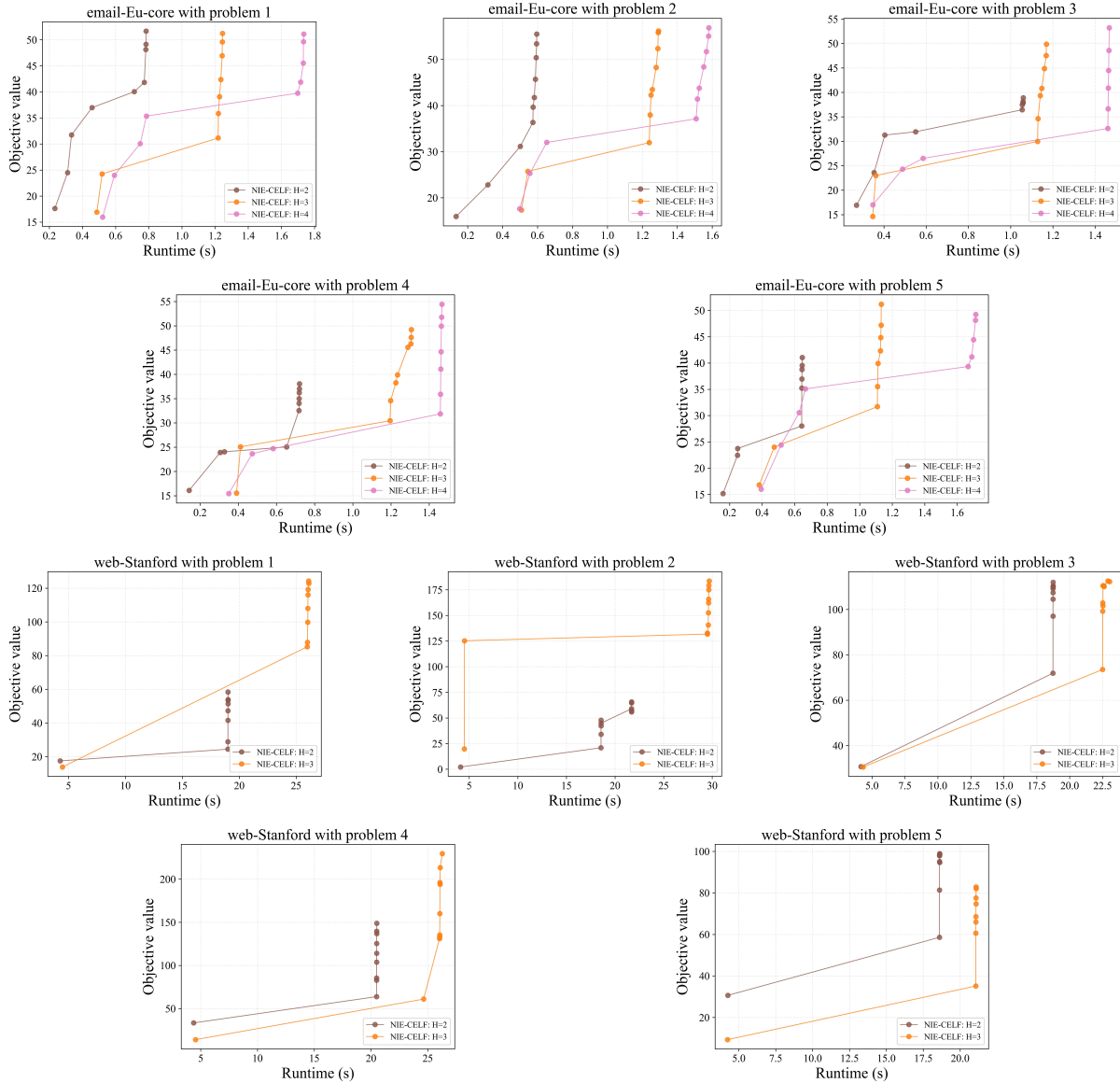


Fig. 5. The objective value achieved by NIE-CELF under different values of H .

of nodes and edges. As an evaluation approach for the blocked influence, NIE can be readily combined with existing IBM optimization algorithms such as the greedy algorithm. Experiments on 25 IBM problems involving up to 280,000 nodes and 2,300,000 edges show that the NIE-based optimization method significantly outperforms the state-of-the-art methods in terms of both computational time and solution quality (given a time budget of one minute). Particularly, the NIE-based optimization method is suitable to cases where high-quality solutions to large-scale IBM problems need to be obtained in seconds.

The promising performance of NIE suggests several potential directions for future research. Firstly, to achieve even higher computational efficiency, it is possible to combine NIE with end-to-end solution prediction methods [33] or a portfolio of different optimization methods [34]–[36]. Secondly, representation learning modules for graph, e.g., graph neural

networks, might be employed to substitute the current feature extractor in NIE. Lastly, it is also interesting to investigate on leveraging graph contrastive learning [37] and active learning [38] to reduce the amount of labeled data for training NIE.

APPENDIX A COMPLEXITY ANALYSIS FOR HMP*

HMP* first generates l R-samples by running Algorithm 1 in [10] and collects $\mathcal{R}_l = \{\mathcal{P}_1, \dots, \mathcal{P}_l\}$ where \mathcal{P}_i is a family of the subsets of V for $i = 1, \dots, l$. Then, the blocked influence is estimated by Eq. (3).

$$\hat{f}(S_t|S_f) = \frac{\sum_{P \in \mathcal{R}_l} \sum_{P \in \mathcal{P}} y(P, S_t)}{l}, \quad (3)$$

where $y(P, S_t)$ equals to 1 if $P \cap S_t \neq \emptyset$ otherwise 0.

From Algorithm 1 in [10] and Eq. (3), it is inferred that the worst-case time complexity to estimate the blocked influence

is $\mathcal{O}(l \cdot k_t \cdot \min(m, n))$ because the size of \mathcal{P} is bounded by m and n and the worst-case time complexity for computing $y(P, S_t)$ is $\mathcal{O}(k_t)$.

APPENDIX B

COMPLEXITY ANALYSIS FOR STRATLEARNER*

The key idea of StratLearner* is to calculate the sum of the weighted scores of S_t on t subgraphs. The estimated blocked influence given S_f and S_t is computed as follows [11].

$$\hat{f}(S_t|S_f) = \sum_{i=1}^t w_i \sum_{v \in V} f_{g_i}^v(S_f, S_t|\emptyset) \quad (4)$$

where $w_i (i = 1, \dots, t)$ is the predefined weight. Define $d_g(S, v) = \min_{u \in S} d_g(u, v)$ where $d_g(u, v)$ is the shortest distance from u to v given a graph g . $f_{g_i}^v(S_f, S_t|\emptyset)$ equals to 1 if $d_{g_i}(S_t, v) < d_{g_i}(S_f, v)$ and $d_{g_i}(S_f, v) \neq \infty$ otherwise 0 given g_i for $i = 1, \dots, t$.

Eq. (4) reveals that the worst-case time complexity is $\mathcal{O}(t \cdot (k_f + k_t) \cdot n)$ if $d_g(S, v)$ is selected by the BFPRT algorithm [30].

REFERENCES

- [1] World Economic Forum, "Global risks report 2023," [Online]. Available: https://www3.weforum.org/docs/WEF_Global_Risks_Report_2023.pdf.
- [2] A. Zareie and R. Sakellariou, "Minimizing the spread of misinformation in online social networks: A survey," *Journal of Network and Computer Applications*, vol. 186, p. 103094, 2021.
- [3] Homeland Security of U.S. Department, [Online]. Available: <https://www.dhs.gov/publication/st-frg-countering-false-information-social-media-disasters-and-emergencies>, 2022.
- [4] United Nations, [Online]. Available: <https://www.un.org/zh/coronavirus/five-ways-united-nations-fighting-infodemic-misinformation>, 2022.
- [5] C. Budak, D. Agrawal, and A. El Abbadi, "Limiting the spread of misinformation in social networks," in *Proceedings of the 20th International Conference on World Wide Web*, 2011, pp. 665–674.
- [6] W. Chen, C. Wang, and Y. Wang, "Scalable influence maximization for prevalent viral marketing in large-scale social networks," in *Proceedings of the 16th ACM SIGKDD International Conference on Knowledge Discovery and Data Mining*, 2010, pp. 1029–1038.
- [7] D. Kempe, J. Kleinberg, and É. Tardos, "Maximizing the spread of influence through a social network," in *Proceedings of the Ninth ACM SIGKDD International Conference on Knowledge Discovery and Data Mining*, 2003, pp. 137–146.
- [8] J. Leskovec and A. Krevl, "Snap datasets: Stanford large network dataset collection." [Online]. Available: <http://snap.stanford.edu/data>, 2014.
- [9] Q. He, Y. Lv, X. Wang, M. Huang, and Y. Cai, "Reinforcement learning-based rumor blocking approach in directed social networks," *IEEE Systems Journal*, vol. 16, no. 4, pp. 6457–6467, 2022.
- [10] G. A. Tong and D.-Z. Du, "Beyond uniform reverse sampling: A hybrid sampling technique for misinformation prevention," in *IEEE INFOCOM 2019-IEEE Conference on Computer Communications*. IEEE, 2019, pp. 1711–1719.
- [11] G. Tong, "Stratlearner: Learning a strategy for misinformation prevention in social networks," *Advances in Neural Information Processing Systems*, vol. 33, pp. 15 546–15 555, 2020.
- [12] J. Leskovec, A. Krause, C. Guestrin, C. Faloutsos, J. VanBriesen, and N. Gance, "Cost-effective outbreak detection in networks," in *Proceedings of the 13th ACM SIGKDD International Conference on Knowledge Discovery and Data Mining*, 2007, pp. 420–429.
- [13] P. Wu and L. Pan, "Scalable influence blocking maximization in social networks under competitive independent cascade models," *Computer Networks*, vol. 123, pp. 38–50, 2017.
- [14] X. He, G. Song, W. Chen, and Q. Jiang, "Influence blocking maximization in social networks under the competitive linear threshold model," in *Proceedings of the 2012 Siam International Conference on Data Mining*. SIAM, 2012, pp. 463–474.
- [15] Y. Li, J. Fan, Y. Wang, and K.-L. Tan, "Influence maximization on social graphs: A survey," *IEEE Transactions on Knowledge and Data Engineering*, vol. 30, no. 10, pp. 1852–1872, 2018.
- [16] C. Borgs, M. Brautbar, J. Chayes, and B. Lucier, "Maximizing social influence in nearly optimal time," in *Proceedings of the Twenty-fifth Annual ACM-SIAM Symposium on Discrete Algorithms*. SIAM, 2014, pp. 946–957.
- [17] W. Hong, C. Qian, and K. Tang, "Efficient minimum cost seed selection with theoretical guarantees for competitive influence maximization," *IEEE Transactions on Cybernetics*, vol. 51, no. 12, pp. 6091–6104, 2020.
- [18] C. Song, W. Hsu, and M. L. Lee, "Temporal influence blocking: Minimizing the effect of misinformation in social networks," in *2017 IEEE 33rd International Conference on Data Engineering*. IEEE, 2017, pp. 847–858.
- [19] G. Tong, W. Wu, L. Guo, D. Li, C. Liu, B. Liu, and D.-Z. Du, "An efficient randomized algorithm for rumor blocking in online social networks," *IEEE Transactions on Network Science and Engineering*, vol. 7, no. 2, pp. 845–854, 2017.
- [20] R. Yan, D. Li, W. Wu, D.-Z. Du, and Y. Wang, "Minimizing influence of rumors by blockers on social networks: algorithms and analysis," *IEEE Transactions on Network Science and Engineering*, vol. 7, no. 3, pp. 1067–1078, 2019.
- [21] H. Zhang, H. Zhang, X. Li, and M. T. Thai, "Limiting the spread of misinformation while effectively raising awareness in social networks," in *Computational Social Networks: 4th International Conference, CSoNet 2015, Beijing, China, August 4-6, 2015, Proceedings 4*. Springer, 2015, pp. 35–47.
- [22] W. Chen, S. Gao, W. Chen, and J. Du, "Optimizing resource allocation in service systems via simulation: A bayesian formulation," *Production and Operations Management*, vol. 32, no. 1, pp. 65–81, 2023.
- [23] W. Chen, H. Guo, and K.-L. Tsui, "An adaptive gaussian process-based search for stochastically constrained optimization via simulation," *IEEE Transactions on Automation Science and Engineering*, vol. 18, no. 4, pp. 1718–1729, 2020.
- [24] W. Chen, W. Hong, H. Zhang, P. Yang, and K. Tang, "Multi-fidelity simulation modeling for discrete event simulation: An optimization perspective," *IEEE Transactions on Automation Science and Engineering*, 2022.
- [25] W. Chen, H. Guo, and K.-L. Tsui, "A new medical staff allocation via simulation optimisation for an emergency department in hong kong," *International Journal of Production Research*, vol. 58, no. 19, pp. 6004–6023, 2020.
- [26] S. Liu, K. Tang, and Y. Xin, "On performance estimation in automatic algorithm configuration," in *Proceedings of the 34th AAAI Conference on Artificial Intelligence*, 2020, pp. 2384–2391.
- [27] X. Lu, T. Sun, and K. Tang, "Evolutionary optimization with hierarchical surrogates," *Swarm and Evolutionary Computation*, vol. 47, pp. 21–32, 2019.
- [28] M. Zhang, H. Li, S. Pan, J. Lyu, S. Ling, and S. Su, "Convolutional neural networks-based lung nodule classification: A surrogate-assisted evolutionary algorithm for hyperparameter optimization," *IEEE Transactions on Evolutionary Computation*, vol. 25, no. 5, pp. 869–882, 2021.
- [29] NetworkX Developers, [Online]. Available: <https://networkx.org/documentation/latest/index.html#>.
- [30] M. Blum, R. W. Floyd, V. R. Pratt, R. L. Rivest, R. E. Tarjan *et al.*, "Time bounds for selection," *Journal of Computer and System Sciences*, vol. 7, no. 4, pp. 448–461, 1973.
- [31] R. J. Lewis, "An introduction to classification and regression tree (cart) analysis," in *Annual Meeting of the Society for Academic Emergency Medicine in San Francisco, California*, vol. 14. Citeseer, 2000.
- [32] J. Kleinberg, "The small-world phenomenon: An algorithmic perspective," in *Proceedings of the Thirty-second Annual ACM Symposium on Theory of Computing*, 2000, pp. 163–170.
- [33] S. Liu, Y. Zhang, K. Tang, and X. Yao, "How good is neural combinatorial optimization? A systematic evaluation on the traveling salesman problem," *IEEE Computational Intelligence Magazine*, vol. 18, no. 3, pp. 14–28, 2023.
- [34] S. Liu, K. Tang, and X. Yao, "Automatic construction of parallel portfolios via explicit instance grouping," in *Proceedings of the AAAI Conference on Artificial Intelligence*, 2019, pp. 1560–1567.
- [35] K. Tang, S. Liu, P. Yang, and X. Yao, "Few-shots parallel algorithm portfolio construction via co-evolution," *IEEE Transactions on Evolutionary Computation*, vol. 25, no. 3, pp. 595–607, 2021.
- [36] S. Liu, K. Tang, and X. Yao, "Generative adversarial construction of parallel portfolios," *IEEE Transactions on Cybernetics*, vol. 52, no. 2, pp. 784–795, 2022.

- [37] J. Wu, W. Fan, J. Chen, S. Liu, Q. Li, and K. Tang, "Disentangled contrastive learning for social recommendation," in *Proceedings of the 31st ACM International Conference on Information & Knowledge Management, Atlanta, GA, USA, October 17-21, 2022*, 2022, pp. 4570–4574.
- [38] R. He, S. Liu, S. He, and K. Tang, "Multi-domain active learning: Literature review and comparative study," *IEEE Transactions on Emerging Topics in Computational Intelligence*, vol. 7, no. 3, pp. 791–804, 2023.